Kochi Chapter

Indian Geotechnical Conference
IGC 2022
15th – 17th December, 2022, Kochi

Application of Geogrid for the Rock-Soil Interface Stability in Railway Embankments

T. I George [1], Amit Bhimrao Somwanshi [2] and SandeepMangal Ghan [3]

[1 2 3]Transportation Infrastructure IC, EDRC (RREC), L & T Construction,
Mumbai 400093, India
george.idiculla@lntecc.com

Abstract. Geogrid has been used for the last few decades mainly as a reinforcing material. The application of geogrid in railway embankment formation to lessen the settlement and thereby stress is well addressed by researchers. This literature explores the application of geogrid to arrest the possible shear failure at the rock-soil interface in deep rock cuts for the formation of high railway embankments. The geogrid is fixed to the rock-cut face using anchors and plates with adequate overlap. This provision of geogrids will avoid the requirement of berm formations for the interface stability and this in turn evades the toe cutting of rock mass which may affect global stability. An extensive parametric study is performed by numerical modelling of railway embankments at deep cut rocks using the finite element tool, PLAXIS 2D. The strength and other parameters of geogrid required for this application are decided by numerical studies and are recommended for field implementation.

Keywords: Geogrid, Rock-Soil Interface; High Embankments; Deep Cuts.

1 Introduction

Rapid urbanization demands the expansion of railway networks, the principal mode of transportation for freight and passengers in India. A stretch of around 3 kilometers requires deep rock cuts of nearly 50 m, for the construction of a new railway alignment. Railway embankments of heights ranging from 15 m to 25 m are proposed on the overall stretch. The stability analyses are performed for the rock cut slopes against all possible failures, viz. toppling, planar sliding and wedge failure. In view of critical analyses, no further toe cutting is advised on the rock-cut slopes which restricts the possibility of bench formations to arrest the shear failure at the rock-soil interface. This leads to the implementation of a typical geosynthetics material, geogrid on embankment fill to overcome the shear failure at the rock-soil interface.

Geogrids are widely used in transportation infrastructure due to their high strength, stability and deformability [1-3]. In the case of soft foundations, embankments and retaining walls geogrids have already proven effective in increasing the tensile strength of soil structures [3-9]. The enhanced interfacial properties in the reinforced soil help to achieve enhanced bearing capacity, resilient modulus and deformation resistance. However, this literature moves away from the traditional usage of geogrid and focuses on

its application in railway engineering mainly targeting to arrest the possible shear failure at the rock-soil interface.

For its field application, the length, strength and spacing of geogrids to be used are to be investigated. A systematic study on this area is required to understand its effectiveness in minimizing the shear failure at the rock-soil interface. Laboratory and field experiments on the same can be time-consuming and costly. Also, the data obtained from the experiments alone are limited and not sufficient to conclude the understanding and proceed with field implementation. On the other side numerical modelling is more convenient in generating desired data and can be used to understand the proper behaviour and mechanism, if properly validated. The present study explains numerical study using a finite element tool, Plaxis 2D, on geogrids used at the rock-soil interface. In the first phase, the numerical model is validated with some centrifuge experiment results (from literature) of a similar application. Afterward, extensive parametric studies are performed to understand the overall mechanism. The study concludes with the case-specific design parameters to be used in the field, as well as findings in general.

2 Numerical Model

2.1 Validation

Zhang et al. 2022 [10] studied the reinforcement effect of geogrids in the junction between new and existing subgrades in highway widening. This research group performed centrifugal tests in high gravity environments (at 60 g) (Fig. 1 shows a schematic representation of the centrifuge model), to simulate the field dimension and the outcome of the research was the field implementation of geogrid in widening a highway in China. Hence the present study also aims for a similar application of geogrid, this centrifuge experiment results are taken for the validation of numerical models. The centrifuge experiment (or highway widening using geogrids) is replicated numerically in 19 stages as given in Table 1. The important stages are shown in Fig. 2.

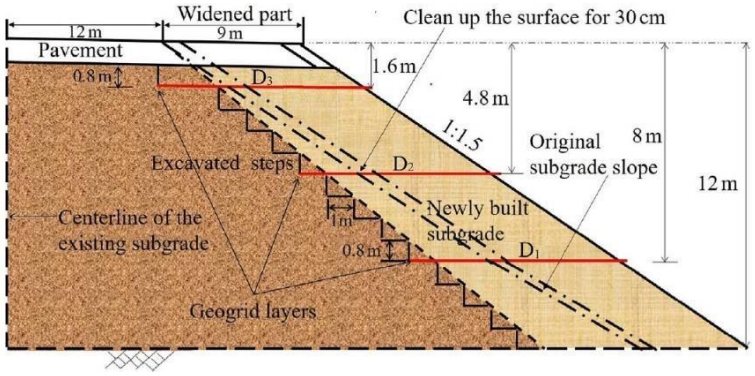

Fig. 1. Schematic representation of highway widening (centrifuge model).

Table 1. Stages of numerical model simulating centrifuge test.

Stage 0		Application of foundation soil conditions
Stage 1	Stage 11*	Filling of subgrade layer 1 (*and paving 1st layer geogrid)
Stage 2	Stage 12	Consolidation for 14 days
Stage 3	Stage 13*	Filling of subgrade layer 2 (*and paving 2nd layer geogrid)
Stage 4	Stage 14	Consolidation for 14 days
Stage 5	Stage 15*	Filling of subgrade layer 3 (*and paving 3nd layer geogrid)
Stage 6	Stage 16	Consolidation for 14 days
Stage 7	Stage 17	Pavement fill
Stage 8	Stage 18	Consolidation for 14 days
Stage 9	Stage 19	Traffic operation (applying 10 kPa load for 5475 days)
Stage 10		Cutting and excavation of steps (riser: 0.8 m and tread: 1 m)

The material parameters (shown in Table 2) used in the model were obtained from the field test, laboratory consolidation test, and direct shear test [10]. Three layers of geogrids are used named from the bottom as D1, D2 and D3. Fig. 3 illustrates the strains observed at each geogrid layer in the present numerical study. It also portrays the closeness of observed numerical results to the values obtained from the centrifuge model study. The numerical model is thus validated, and further extensive parametric studies are performed on the application of geogrids at the rock-soil interface.

Table 2. Material properties (After Zhang et al. 2022).

Layer material	Elastic modulus (MPa)	Poisson ratio	Density (kg/m^3)	Cohesive force (kPa)	Friction angle (°)
Pavement	1200	0.2	2300	…..	….
Subgrade	20.75	0.25	1870	13.4	32.1
Foundation	6.67	0.35	1920	2.28	26

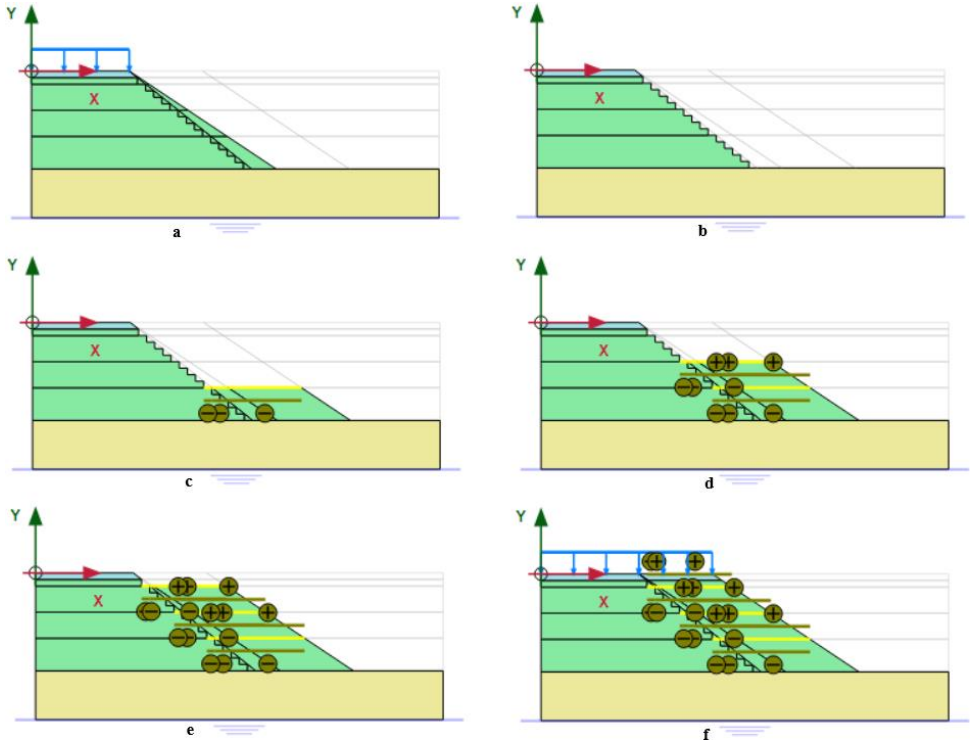

Fig. 2. Numerical model(**a**:Stage 9, **b**:Stage 10, **c**:Stage 11, **d**:Stage 13, **e**:Stage 15, **f**:Stage 19)

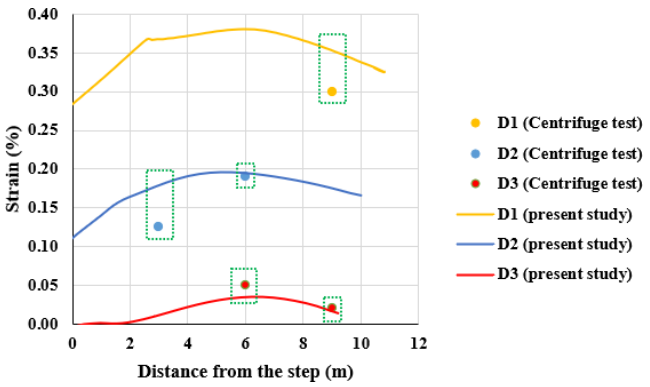

Fig. 3. Strains on geogrids: Numerical (present study) and experiment results (Zhang et al. 2022).

2.2 Geogrids for rock-soil interface

For the construction of railway embankments of up to 20 m in height, it is proposed to fill it in layers with geogrids to minimize the sliding of soil at the rock-soil interface. Fig. 4 is the photograph of the existing condition of one stretch at the project site showing the exposed rock cut. Almost half of the height of the rock-cut slope is to be filled

for railway embankment construction. The application of geogrids (properly anchored to rock face) in embankment layers is imperative as no further toe cutting is advised considering the stability aspects.

Fig. 4. Photograph of a stretch at the project site showing exposed rock cut face.

A critical section along the whole stretch of the project is considered and is modelled in Plaxis 2D (Fig. 5). Construction sequences at the site are simulated in numerical modelling and are analyzed stagewise, viz. initial rock cut slope, layer by layer filling of embankment fill (with and without geogrid placement), modelling subgrade, ballast, sleepers and finally applying railway load. The material properties used in the numerical modelling are determined from laboratory tests and are given in Table 3. To identify the effect of geogrid various points A1 to A9 (at 3 m vertical distance) at the rock-soil interface is marked in the numerical model to check the slippage (relative vertical displacement) of soil. Geogrids are anchored to the rock face using rock anchors as shown in Fig. 6. 32 mm dia CRS (corrosion resistance steel) are modelled as rock bolts using embedded beam element (enabling rock bolt behaviour), in Plaxis. The anchors are inserted 2 m inside the rock mass at 20 degrees inclination with horizontal. The rock bolts are modelled from a node on geogrid to ensure proper connection between geogrid and rock bolt. An overlapping length (i.e., length of geogrid on rock face from the connection joint/node) of 0.5 m is provided.

Table 3. Material properties used in numerical modelling.

Material	Constitutive model	Young's modulus (kPa)	Unit weight (kN/m^3)	Poisson ratio	Uniaxial compressive strength (kPa)	Cohesion (kPa)	Friction angle (°)
Poor rock	Hoek-Brown	56.59x10^3	26.3	0.2	88.77x10^3		
Intermediate rock	Hoek-Brown	32.19x10^5	26.5	0.2	131.6x10^3		
Strong rock	Hoek-Brown	21.83x10^6	26.67	0.2	172.8x10^3		
Embankment fill	Mohr-Coulomb	40x10^3	17	0.3		7.2	31

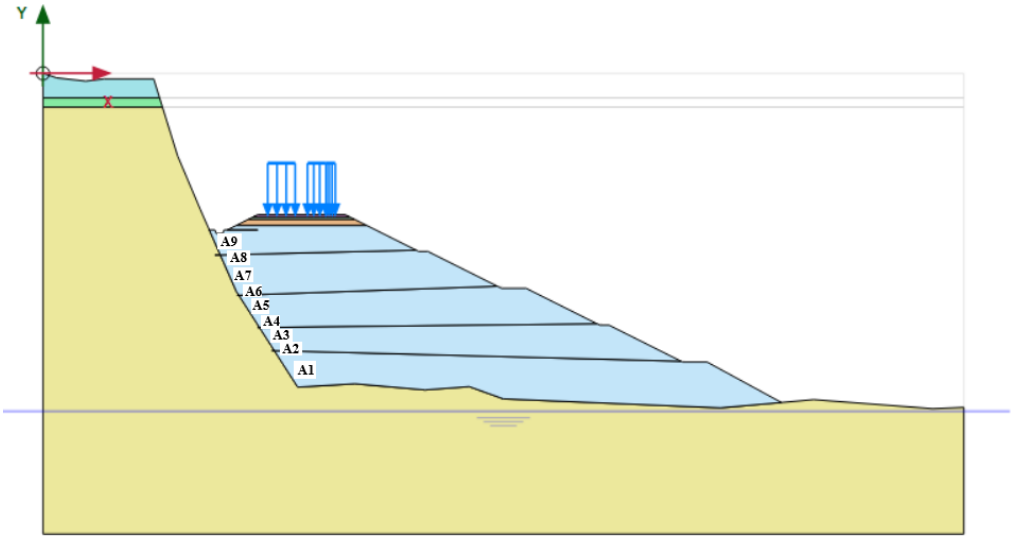

Fig. 5. Numerical modelling of a critical section of high embankment on rock cut slope.

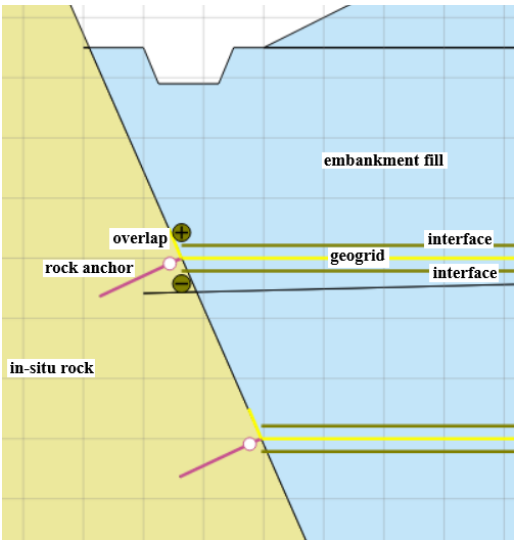

Fig. 6. Numerical model showing anchoring of geogrid layers on the rockface.

3 Parametric Study

To identify the effect of geogrid, various points A1 to A9 (at 3 m vertical distance) at the rock-soil interface are marked in the numerical model to check the slippage (relative vertical displacement) of soil. Geogrid layers with 3 m vertical spacing are named G1 to G7 from bottom to top of the embankment fill. Parametric analyses are performed by considering different cases as mentioned in Table 4.

Table 4. Parametric studies.

Case	Specifications	Length of geogrid (m)	Vertical spacing between geogrids (m)	Activated geogrid layers in Numerical model
Case 1	Embankment fill without geogrid	….	…	
Case 2	Embankment fill with 7 layers of geogrid	Full length	3	G1-G7
Case 3	Embankment fill with 3 layers of geogrid	Full length	9	G1, G4 and G7
Case 4	Embankment fill with 3 layers of geogrid	Full length	6	G2, G4 and G6
Case 5	Embankment fill with 3 layers of geogrid	15 m	6	G2, G4 and G6
Case 6	Embankment fill with 3 layers of geogrid	7 m	6	G2, G4 and G6

3.1 Design Considerations

Fig. 7 shows the relative vertical displacements of points A1 to A9 for different cases of geogrid applications. The values shown are at the final stages after simulating the railway live load. Shear displacements at no geogrid case are minimized by an average of 80% by the application of geogrid, keeping them well within the permissible limits. This indicates the relevance of implementing geogrid to arrest the shear failure at the

rock-soil interface. The main outcome of this parametric study is to finalize the design considerations, mainly length, vertical spacing and strength of geogrid.

Vertical spacing

The shear displacements at Case 2 (embankment fill with 7 layers of geogrid, with vertical spacing 3 m) are minimum whereas the same at Case 3 (embankment fill with 3 layers of geogrid, with vertical spacing 9 m) exceeds the permissible limits. In comparison with Case 2, Case 4 (embankment fill with 3 layers of geogrid, with vertical spacing 6 m) is more economical. Also, the shear displacements observed at points A1 to A2 are significantly reduced. This points to the consideration of vertical spacing between the geogrid layers as 6 m in the field application.

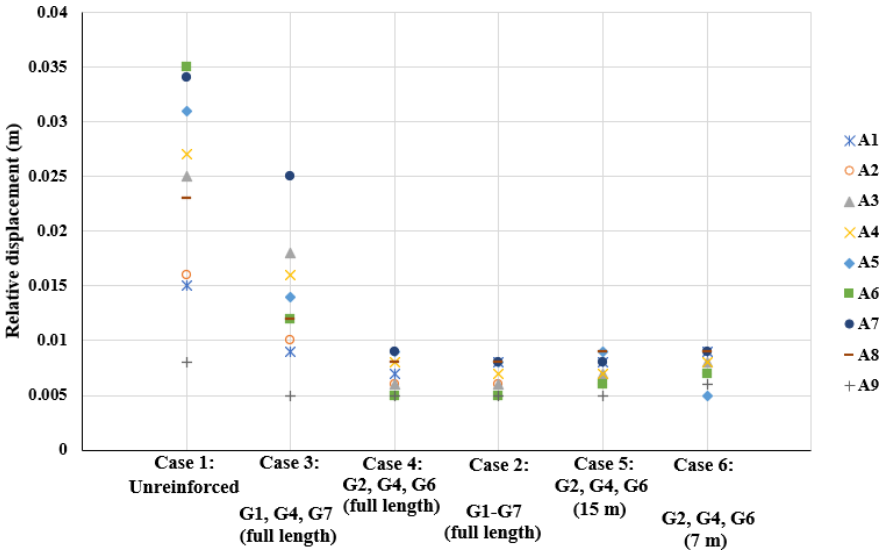

Fig. 7. Shear displacements at rock-soil interface.

Length

Fig. 8 to 12 show the axial force mobilized on the geogrid layers at the final stage of railway loading. The mobilized axial force is maximum at the rock-soil interface, and it decreases along its length. Furthermore, it is observed that the mobilized axial force dies downs after around 5-6 m in each layer. These observations are further examined and confirmed with decreased length of geogrid layers (15 m in Case 5 and 7 m in Case 6). In these investigations, it is examined that the mobilized axial forces and the extent to which they are mobilized will not change significantly as the geogrid lengths are reduced up to 7 m. This indicates further increases in the length of geogrid layers are not going to contribute to the stability aspect at the rock-soil interface. Though the extent of mobilized axial force is up to maximum 6 m from the rock face, considering other precautional aspects, the length of geogrid layers for filed implementation is considered as 7 m.

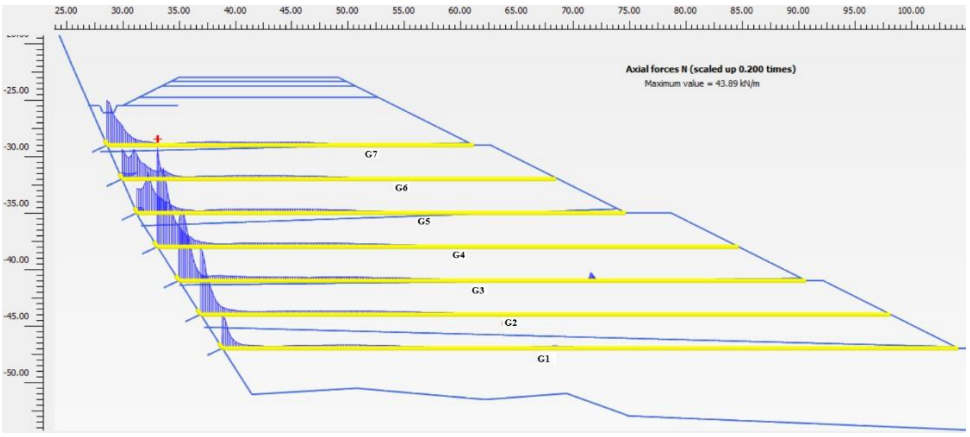

Fig. 8. Case 2: Mobilized axial force on geogrid layers.

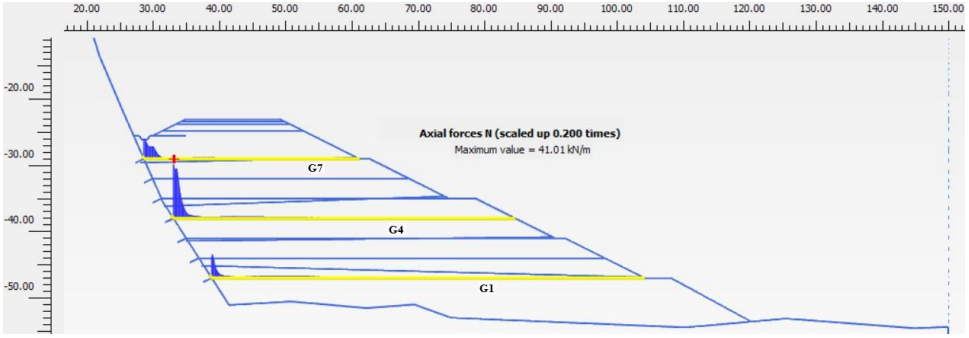

Fig. 9. Case 3: Mobilized axial force on geogrid layers.

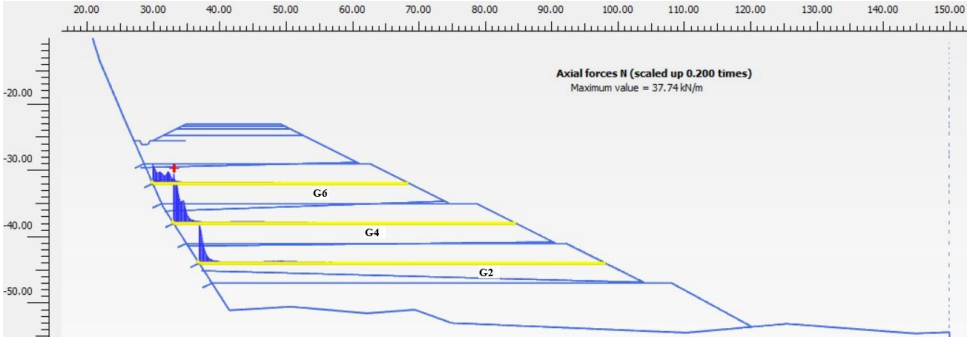

Fig. 10. Case 4: Mobilized axial force on geogrid layers.

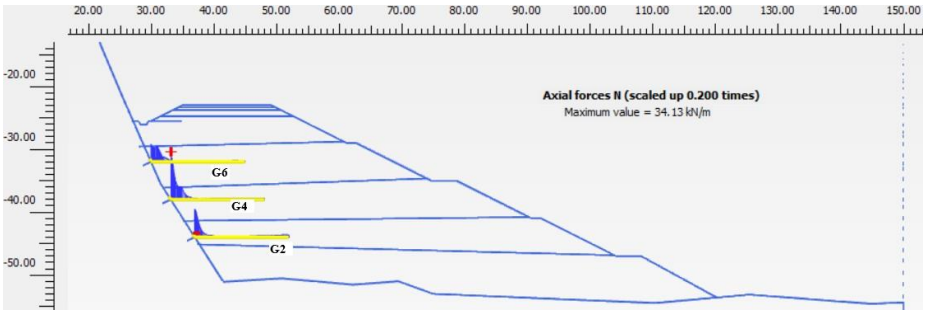

Fig. 11. Case 5: Mobilized axial force on geogrid layers.

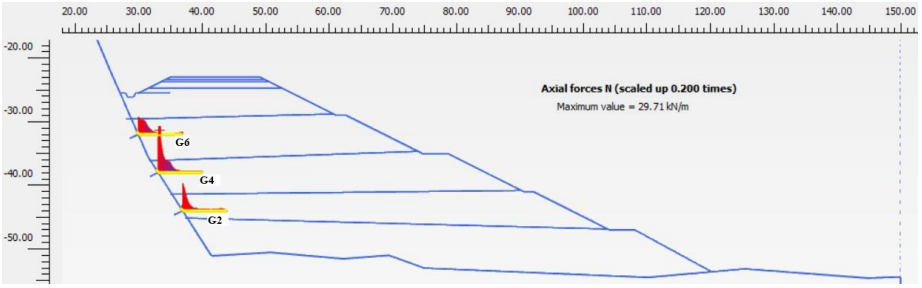

Fig. 12. Case 6: Mobilized axial force on geogrid layers.

Strength

Fig. 13 illustrates the maximum axial force mobilized on geogrid layers at the final stage of railway loading. In all the cases considered the maximum axial force is mobilized on G4. This highlights the position of G4 as very pertinent. The maximum mobilized axial force being around 45 kN/m and the average being 25 kN/m, it is recommended to use uniaxial geogrid of the ultimate strength of 100 kN/m.

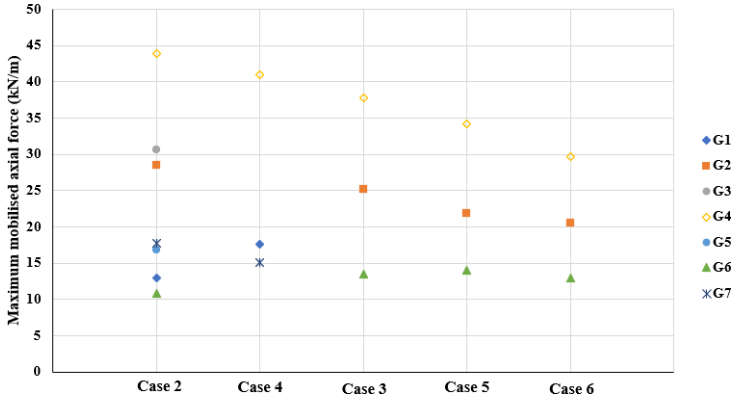

Fig. 13. Maximum mobilized axial force on geogrid layers.

4 Conclusion

Based on the criticality of the project and the stability of rock slopes being a major concern, further excavation in nearby rock slopes is prohibited owing to which the susceptible interface shear failure at high embankment needs to be arrested with geogrids. As the field application of this particular case is very limited and the experimental studies on this are more tedious, numerical analyses are performed to study the effect of geogrid on minimizing the shear displacement at the rock-soil interface. Extensive parametric studies are performed, and the results are incorporated to determine the design considerations for the field application on an existing railway project. The following are the main conclusions from the study.

i. The vertical spacing of the geogrid layers to minimize the shear failure is optimized to 6 m.
ii. The length of geogrid is confirmed as 7 m, beyond which there is no effect.
iii. The ultimate strength of the geogrid layers to be used in the field is determined as 100 kN/m.

References

1. Xiao, Y., He, X., Evans, M., Stuedlein, A. W., Liu. H.: Unconfined Compressive and Splitting Tensile Strength of Basalt Fiber-Reinforced Biocemented Sand. Journal of Geotechnical and Geoenvironmental Engineering 145, no. 9, 04019048, https://doi.org/10.1061/(ASCE)GT.1943-5606.0002108 (2019).
2. Kwon, J., Tutumluer, E.: Geogrid Base Reinforcement with Aggregate Interlock and Modeling of Associated Stiffness Enhancement in Mechanistic Pavement Analysis. Transportation Research Record: Journal of the Transportation Research Board 2116, no. 1, pp.85-95, https://doi.org/10.3141/2116-12 (2009).
3. Tutumluer, E., Huang, H., Bian, X.: Geogrid-Aggregate Interlock Mechanism Investigated through Aggregate Imaging-Based Discrete Element Modeling Approach. International Journal of Geomechanics 12, no. 4, pp. 391-398, https://doi.org/10.1061/(asce)gm.1943-5622.0000113 (2012).
4. Abu-Farsakh, M., Hanandeh, S., Homammad, L., Chen, Q.: Performance of Geosynthetic Reinforced/Stabilized Paved Roads Built over Soft Soil under Cyclic Plate Loads. Geotextiles and Geomembranes 44, no. 6, pp. 845-853, https://doi.org/10.1016/j.geotexmem.2016.06.009 (2016).
5. Cui, W., Xiao, M.: Centrifuge Modeling of Geogrid-Reinforced and Rammed Soil-Cement Column-Supported Embankment on Soft Soil. Journal of Testing and Evaluation 48, no. 5, pp. 4016–4029, https://doi. org/10.1520/JTE20170603 (2018).
6. Han, B., Ling, J., Shu, X., Song, W., Boudreau, R. L., Hu. W., Huang, B.: Quantifying the Effects of Geogrid Reinforcement in Unbound Granular Base. Geotextiles and Geomembranes 47, no. 3, pp. 369–376, https:// doi.org/10.1016/j.geotexmem.2019.01.009 (2019).
7. Correia, N. S., Esquivel, E. R., Zornberg, J. G.: Finite-Element Evaluations of Geogrid-Reinforced Asphalt Overlays over Flexible Pavements. Journal of Transportation Engineering, Part B: Pavements 144, no. 2, 04018020, https://doi.org/10.1061/JPEODX.0000043 (2018).
8. Zheng, B., Huang, X., Zhao, R., Chen, J., Zhang, W., Yu, T.: Sensitivity Analysis of Distress Influence Factors on Steel-Plastic Compound Reinforced Retaining Wall. Journal of Testing and Evaluation 48, no. 6, pp. 4699–4718, https://doi.org/10.1520/JTE20180632 (2019).

9. Hang, B., Ling, J., Shu, X., Gong, H., Huang, B.: Laboratory Investigation of Particle Size Effects on the Shear Behavior of Aggregate-Geogrid Interface. Construction and Building Materials 158, pp. 1015–1025, https://doi.org/10. 1016/j.conbuildmat.2017.10.045 (2018).
10. Zhang, J., Li, X., Ding, L., Xiao, Y.: Reinforcement Effect Investigation of Geogrids in the Junction between New and Existing Subgrades in Highway Widening. Journal of Testing and Evaluation. doi:10.1520/JTE20210223: (2022)